

## Solid-fluid transition and cell sorting in epithelia with junctional tension fluctuations Supplemental Material

Matej Krajnc<sup>1,2</sup>

<sup>1</sup>*Jožef Stefan Institute, Jamova 39, SI-1000 Ljubljana, Slovenia*

<sup>2</sup>*Lewis-Sigler Institute for Integrative Genomics,  
Princeton University, Washington Road, Princeton NJ 08540, USA*

### I. APE MODEL WITH TENSION FLUCTUATIONS

To directly compare some of the results reported in the main text with the models which assume a preferred cell perimeter  $q_0$ , we implemented the Area- and Perimeter-elasticity (APE) model with tension fluctuations. Like in the pure tension-based model, vertices in the APE model undergo a friction dominated dynamics  $\dot{\mathbf{r}}_i = -\nabla_i W$ , where the APE energy functional in dimensionless form reads

$$W = \sum_{j \in \text{cells}} [k_A(A_j - 1)^2 + (p_j - q_0)^2] + \sum_{j|k} \Delta\gamma_{jk}(t)l_{jk}. \quad (1)$$

Here the first and the second term describe cell-area and cell-perimeter elasticities, respectively, whereas the third term incorporates fluctuations of line tensions, which obey the Ornstein-Uhlenbeck process [Eq. 2 in the main text].

We explored the solid-fluid transition in the  $(q_0, \tau_m, \sigma)$  parameter space (Fig. S1A) by monitoring the mean squared displacements and calculating the effective diffusion coefficients of cell movements  $D_{\text{eff}}$  (Fig. S1B-G). Like in the pure tension-based model,  $D_{\text{eff}}$  measurements at different  $\sigma$  and  $\tau_m$  values collapse when they are plotted against the mean cell-shape index  $\langle q \rangle$ . However, they only collapse if they are evaluated at the same  $q_0$  value (Fig. S1H). The relation  $D_{\text{eff}}(\langle q \rangle)$  is linear and the solid-fluid transition occurs at  $\langle q \rangle \approx 3.81$  for intrinsically jammed tissues ( $q_0 < 3.81$ ). Both observations agree with the pure tension-based model (Fig. 1F of the main text).

Interestingly, at small noise, the (un)jamming transition looks similarly gradual in terms of MSD curves as the one reported in Ref. 20 (Fig. S1B and Fig. 1a in Ref. 20). However, this transition becomes more abrupt at larger values of noise (Fig. S1C) until it disappears at large fluctuations (Fig. S1D). On the other hand, when taking  $\sigma$  as the control parameter, an abrupt transition can be found deep in the solid regime (Fig. S1E) and a more gradual one appears close to the zero-temperature (un)jamming point (Fig. S1F).

Our pure tension-based model can be most directly compared to the APE model deep in the solid regime [e.g.,  $q_0 = 3.5$ ], taking  $\sigma$  as the control parameter. In this case, both models exhibit similarly abrupt transition from caging to diffusive behavior of MSD curves (Fig. S1E and Fig. 1C of the main text)]. This abrupt transition is probably due to an exponential dependance of T1-transition rates on  $1/T_{\text{eff}}$ , where the effective temperature of fluctuations  $T_{\text{eff}}$  is directly related to  $\sigma$  in both models. In particular, at small  $\sigma$  (and thus small  $T_{\text{eff}}$ ) the transition rates are expected to increase very slowly with an increasing  $\sigma$ , however, when  $\sigma$  is sufficiently big, its further increase results in abrupt increases of the rates.

### II. ROUGHNESS OF COMPARTMENTAL BOUNDARIES

We implemented our pure tension-based vertex model on a strip geometry with two (parallel) vertical interfaces between type-1 and type-2 cells (Fig. S2A).

#### *Average dihedral angle*

First, we observed the sharpness of these interfaces by calculating the average cosine of the dihedral angle  $\theta_{m,m+1}$  between two adjacent interface edges (Fig. S2B). We did so both for the differential-adhesion (DA) and the differential-fluctuation (DF) cases:

- In the DA case, we varied the differential tension  $\gamma_a$  at fixed  $\sigma = 0.4$  and  $\tau_m = 0.5$ , which were chosen such that the tissue was fluid. Not too surprisingly, increasing  $\gamma_a$  sharpened the interface (Fig. S2C). This sharpening also showed in  $\langle \cos \theta_{m,m+1} \rangle$ , which approached 1 with the increasing  $\gamma_a$  (Fig. S2D).

- In the DF case, we fixed  $\tau_m = 0.5$  and  $\sigma_- = 0.23$  (i.e., close to the critical value  $\sigma^*$ , which corresponds to the most efficient sorting) while varying  $\sigma_+$ . In contrast to the DA case, where increasing the sorting-promoting parameter,  $\gamma_a$ , also increased  $\langle \cos \theta_{m,m+1} \rangle$ , we found that in the DF case, the sorting-promoting parameter  $\sigma_+$  does not affect  $\langle \cos \theta_{m,m+1} \rangle$  at all and boundaries seem similarly rough at different  $\sigma_+$  values when examined by eye (Fig. S2E,F).

Overall, these results show that while on one hand, the differential adhesion sorts cells into compartmentalized tissues separated by very sharp boundaries, on the other hand, intercompartmental boundaries during differential-fluctuations-driven cell sorting remain rough.

#### *Vanishingly short boundary edges*

The sharpness of intercompartmental boundaries is not solely determined by  $\langle \cos \theta_{m,m+1} \rangle$ , since edges have in general different lengths. Indeed, two adjacent edges can have a large dihedral angle  $\theta_{m,m+1}$ , but if they are both short, they contribute very little to the roughness of the boundary. To quantify this, we extracted the distribution of lengths both for the boundary and bulk edges. In particular, we were interested in the probability of finding vanishingly short edges at the boundary.

- In the DA case, we observed qualitatively similar behavior to the one found within the APE model (Ref. 44). In particular, vanishingly short edges were more probable at higher differential tensions  $\gamma_a$  (Fig. S2G).
- In the DF case, we found the same effect: the probability of finding vanishingly short edges increased with the sorting-promoting parameter  $\sigma_+$  (Fig. S2H). Combined, this result and the fact that  $\langle \cos \theta_{m,m+1} \rangle \approx 1/2$  regardless the value of  $\sigma_+$  (Fig. S2F) probably explain why the intercompartmental boundaries at higher values of  $\sigma_+$  may seem slightly sharper than those at smaller values (Fig. S2E).

## III. SUPPLEMENTARY FIGURES

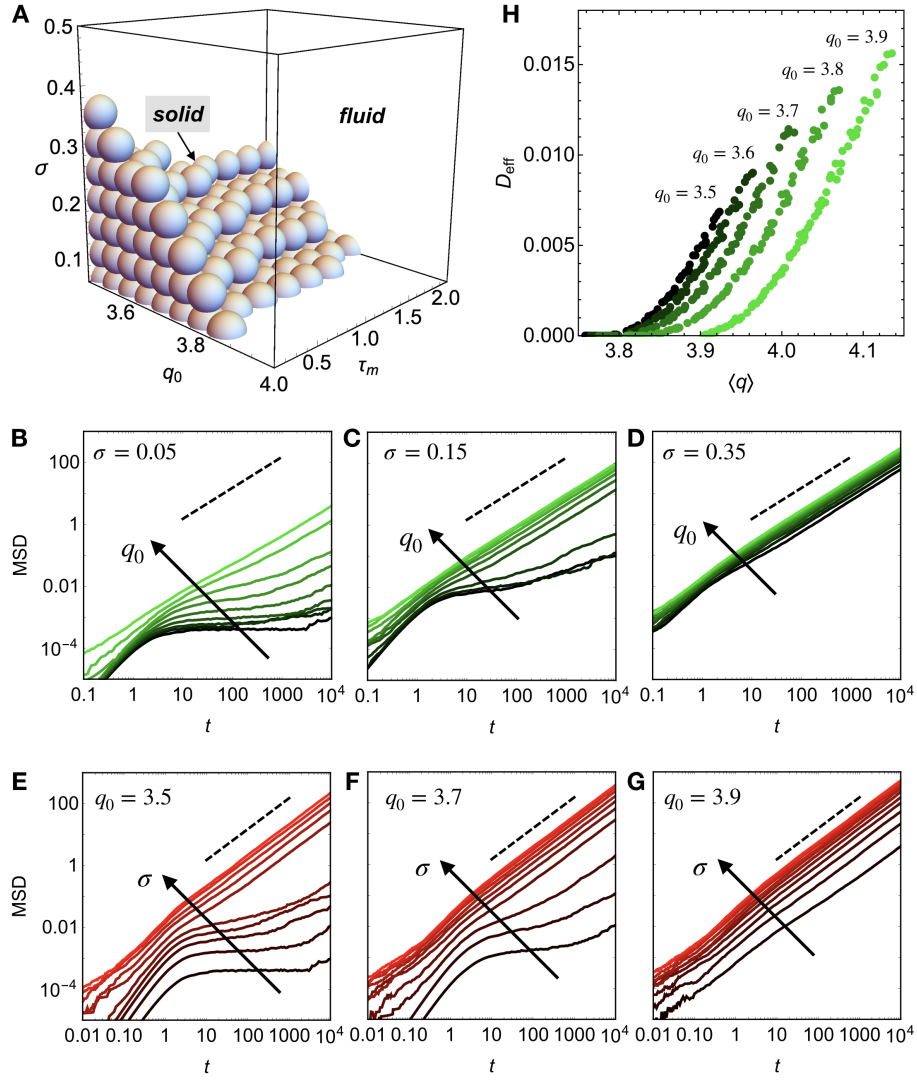


FIG. S1. (A) Phase diagram of solid- and fluid-like tissue behaviors. (B-D) Mean square displacement vs. time at  $\tau_m = 0.75$  and  $\sigma = 0.05, 0.15$ , and  $0.35$  (panels B, C, and D, respectively). (E-G) Mean square displacement vs. time at  $\tau_m = 0.75$  and  $q_0 = 3.5, 3.7$ , and  $3.9$  (panels E, F, and G, respectively). (H) Effective diffusion coefficient plotted vs. the mean cell shape index  $\langle q \rangle$  for different  $\tau_m$  and  $\sigma$  values. The green color scheme in panels B-D and H represent the values of  $q_0$  ( $q_0 = 3.5 - 3.9$ ; from black to light green), whereas the red color scheme in panels E-G represent values of  $\sigma$  ( $\sigma = 0.05 - 0.5$ ).

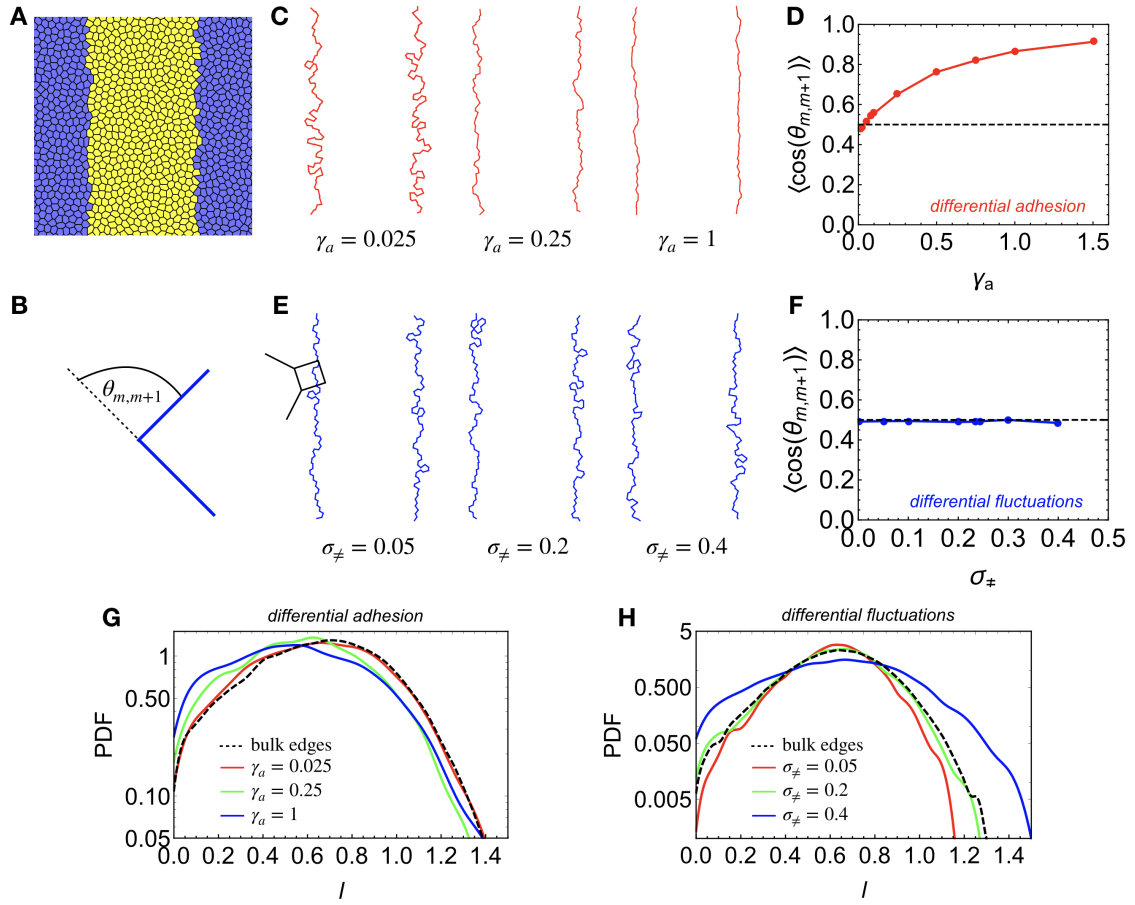


FIG. S2. (A) Simulation snapshot of the strip geometry. Type-1 cells are colored yellow, whereas blue are type-2 cells. (B) Schematic of the dihedral angle  $\theta_{m,m+1}$  between adjacent boundary edges  $m$  and  $m+1$ . (C,E) Boundary shapes at different values of sorting-promoting parameters  $\gamma_a$  and  $\sigma_{\neq}$ . (D,F) Average cosine of the dihedral angle  $\theta_{m,m+1}$  between adjacent boundary edges  $m$  and  $m+1$  as functions of the sorting-promoting parameters  $\gamma_a$  and  $\sigma_{\neq}$ . (G,H) Probability distribution functions of boundary edge lengths at different values of sorting-promoting parameters  $\gamma_a$  and  $\sigma_{\neq}$ . Dashed curves in both cases represent distributions of the bulk edges. Other parameters were set to the following values:  $\tau_m = 0.5$ ,  $\sigma = 0.4$  (panels C, D, and G) and  $\tau_m = 0.5$ ,  $\sigma_{\neq} = 0.23$  (panels E, F, and H).